GOME-2 TOTAL AND TROPOSPHERIC NO_2 VALIDATION BASED ON ZENITH-SKY, DIRECT-SUN AND MULTI-AXIS DOAS NETWORK OBSERVATIONS

G. Pinardi[1], M. Van Roozendael[1], J.-C. Lambert[1], J. Granville[1], F. Hendrick[1], F. Tack[1], H. Yu[1], A. Cede[2,12], Y. Kanaya[3], H. Irie[4], F. Goutail[5], J.-P. Pommereau[5], A. Pazmino[5], F. Wittrock[6], A. Richter[6], T. Wagner[7], M. Gu[7], J. Remmers[7], U. Friess[8], T. Vlemmix[9], A. Piters[10], N. Hao[11], M. Tiefengraber[12,13], J. Herman[2,14], N. Abuhassan[2,14], A. Bais[15], N. Kouremeti[15,21], J. Hovila[16], R. Holla[17], J. Chong[18], O. Postylyakov[19], J. Ma[20]

(1) Belgian Institute for Space Aeronomy (IASB-BIRA), Brussels, Belgium
(2) NASA/Goddard Space Flight Center, GSFC, Greenbelt, MD, USA
(3) Research Institute for Global Change, JAMSTEC, Yokohama, Japan
(4) Center for Environmental Remote Sensing, Chiba University,Chiba, Japan
(5) LATMOS, Laboratoire Atmospheres, Milieux, Observations Spatiales, Guyancourt, France
(6) Institut fur Umweltphysik, Universitat Bremen, Bremen, Germany
(7) Max Planck Institute for Chemistry, Mainz, Germany
(8) Institut fur Umweltphysik, Universitat Heidelberg, Heidelberg, Germany
(9) Department of Geosciences & Remote Sensing, TU-Delft, The Netherlands
(10) Royal Netherlands Meteorological Institute, KNMI, De Bilt, The Netherlands
(11) German Aerospace Center, DLR, Weßling, Germany
(12) LuftBlick, Kreith, Austria
(13) Institute of Meteorology and Geophysics, University of Innsbruck, Austria
(14) University of Maryland, Joint Center for Earth Systems Technology, Baltimore, MD, USA
(15) AUTH, Thessaloniki, Greece
(16) FMI, Helsinki, Finland
(17) DWD, Hohenpeissenberg, Germany
(18) Gwangju Institute of Science and Technology GIST, Gwangju , Korea
(19) Institute of Atmospheric Physics, Russian Academy of Sciences, IAP/RAS, Moscow, Russia
(20) Chinese Academy of Meteorological Sciences,Beijing, China
(21) PhysikalischMeteorologischesObservatorium Davos, World Radiation Center (PMOD/WRC), Davos Dorf, Switzerland

Abstract

Total and tropospheric NO_2 columns have been operationally retrieved from the GOME-2/MetOp instruments since the first MetOp platform was put in orbit in October 2006. GOME-2 NO_2 data products are retrieved in three main steps: (1) a DOAS spectral analysis yielding the total column amount of NO_2 along the slant optical path, (2) an estimation of the stratospheric NO_2 column using tropospheric masking and spatial interpolation, to be subtracted from the total column to derive the tropospheric contribution, and (3) a conversion of the total and tropospheric slant columns into vertical columns based on airmass factor calculations which require a-priori knowledge of the NO_2 vertical distribution and surface albedo, as well as cloud information retrieved from GOME-2 spectra.

In this study we combine correlative measurements available from complementary ground-based remote sensing networks to address the geophysical validation of the GOME-2 NO_2 data products. Zenith-sky DOAS/SAOZ measurements at the usually unpolluted stations of the NDACC network are used to validate the stratospheric NO_2 columns retrieved from the satellite, while direct-sun Pandora and multi-axis MAXDOAS data sets from a number of stations of the NDACC and MADRAS networks are used to investigate the consistency of GOME-2 total and tropospheric NO_2 columns in urban, sub-urban and background conditions. Results are discussed in terms of observed biases between satellite and ground-based data sets, their dependence on location, season and cloud conditions, and for the stratospheric columns, their photochemical effects.

1. GOME-2 NO_2 COLUMN RETRIEVALS

In the framework of the O3M SAF Continuous Development and Operations Phase (CDOP), total, tropospheric and stratospheric NO_2 columns are operationally retrieved from GOME-2 measurements acquired from both MetOp-A and MetOp-B platforms. The detailed GOME-2 GOME Data Processor (GDP) algorithm description can be found in Valks et al. (2011). It is based on a residual technique that involves three steps for the derivation of tropospheric vertical columns (V_t) according to the following equation: $V_t = (S - M_s V_s)/M_t$. First, a total slant column density (S) is retrieved from measured GOME-2 spectra by application of the Differential Optical Absorption Spectroscopy (DOAS, Platt and Stutz, 2008) technique. Secondly the stratospheric content (V_s) is estimated and subtracted from S, and finally the resulting tropospheric slant column is converted into a tropospheric vertical column (V_t) by applying a tropospheric air mass factor (M_t). The tropospheric air mass factor (AMF) calculation requires a-priori knowledge of the NO_2 vertical distribution and surface albedo, as well as cloud information retrieved from GOME-2 spectra.

As part of the operationalization of the GOME-2 NO_2 data products, BIRA-IASB has performed a validation study of both MetOp-A and MetOp-B instruments where the quality of the different components of the level-1-to-2 retrieval chain has been assessed using independent retrieval algorithms and correlative observations performed by ground-based and satellite instruments. Initial and consolidated validation results have been published in successive O3M SAF validation reports (Pinardi et al, 2011, Pinardi et al, 2013). These results are regularly updated on the O3M SAF trace gases Validation & Quality Assessment web server (cdop.aeronomie.be/validation/valid-results). In the present study, we extend the validation of GOME-2 NO_2 data products using a large number of correlative ground-based stations allowing to sample an extended range of atmospheric conditions worldwide. The different geometries of the ground-based instruments are exploited to provide complementary information on atmospheric NO_2.

2. GROUND-BASED INSTRUMENTS

Remote-sensing techniques based on UV-Vis DOAS spectroscopy are particularly well-suited for the validation of tropospheric trace gas observations by satellite sensors (Richter et. al, 2013), because (1) they provide accurate measurements of integrated column amounts (i.e. the quantity measured by space-based instruments), and (2) owing to their remote-sensing nature, they are spatially more representative of satellite observations than e.g. in-situ surface concentrations measured by operational surface monitoring networks.
Different types of ground-based UV-vis DOAS remote-sensing instruments are used in this study to validate the GOME-2 NO_2 column. Depending on the observational geometry (see Figure 1), they are differently sensitive to different vertical parts of the atmosphere and, accordingly, are best suited for the comparison of stratospheric, tropospheric or total content in the atmosphere.

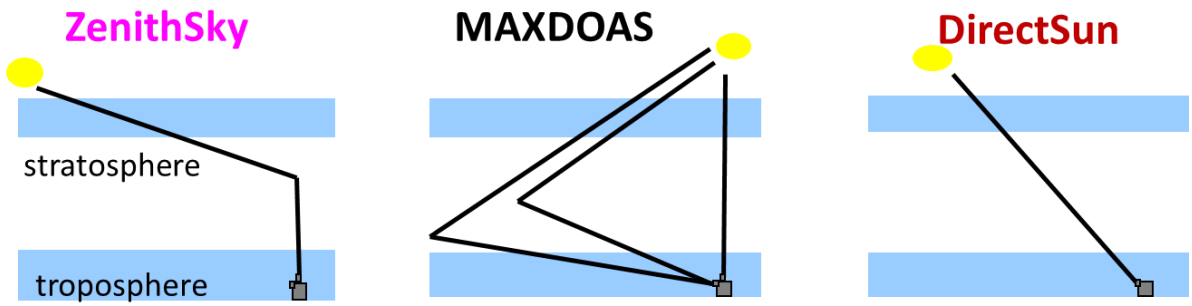

Figure 1: **Illustration of the different observational geometries of the UV-VIS DOAS instruments used in this study.**

2.1 Zenith-sky geometry

Zenith-sky DOAS instruments measure scattered sunlight in the zenith direction (Figure 1a). In this geometry, the solar radiation travels a short path through the troposphere and a longer path through the stratosphere - this effect being extreme at twilight under low sun conditions. Twilight

measurements are thus mainly sensitive to the stratosphere, and provide accurate stratospheric NO_2 column measurements at dusk and dawn (Solomon et al., 1987; Pommereau and Goutail, 1988).
Zenith-sky instruments are part of the NDACC (Network for the Detection of Atmospheric Composition Change) which has provided regular stratospheric NO_2 columns from pole to pole for more than 2 decades, historically at stations with pristine tropospheric air. To ensure consistent long-term measurements, harmonized retrieval strategies have been adopted for use in the network (see Roscoe et al., 1999; Vandaele et al., 2005; Van Roozendael and Hendrick, 2012).
Intercomparison exercises between NDACC certified UV-Vis zenith-sky instruments have shown that NO_2 slant columns (SCD) generally agree within 5% when using standardized analysis procedures (e.g., Roscoe et al., 1999; Vandaele et al. 2005; Roscoe et al. 2010). Total uncertainties on twilight stratospheric vertical columns (VCDs) are dominated by the spectral fit and the AMF calculation. Other systematic sources of uncertainty are related to the NO_2 absorption cross-section and its temperature dependency, as well as the determination of the NO_2 residual amount in the reference spectrum. For the SAOZ instrument largely used in this study, the total random and systematic uncertainties have been estimated to be ~10% and ~20% respectively (Van Roozendael et al., 1994).

2.2 MAXDOAS geometry

Multi-axis DOAS instruments (MAXDOAS) measure scattered sunlight under different viewing elevations from the horizon to the zenith (Figure 1b). The observed light travels a long path in the lower troposphere (the lower the elevation angle, the longer is the path) and the different elevations of one scan have the same path in the stratosphere. The stratospheric contribution can thus be removed by taking the difference in SCD between an off-axis elevation and a zenith reference. Tropospheric absorbers are measured all day long generally up to 85° of solar zenith angle (SZA). In addition, MAXDOAS instruments can provide low resolution vertical profiles (degrees of freedom DOF <3) of NO_2 and aerosol in the lowermost troposphere (Friess et al., 2006; Clemer et al., 2010; Wagner et al., 2011; Irie et al., 2011).
In the past decade, MAXDOAS instruments have been deployed worldwide as part of small research networks, such as the BIRA-IASB (http://uv-vis.aeronomie.be/groundbased/), BREDOM (http://www.doas-bremen.de/groundbased_data.htm), Heidelberg, Mainz and MADRAS (MAX-DOAS instruments in Russia and ASia) networks (Kanaya et al., 2014).
During the EC FP6 GEOMON (Global Earth Observation and Monitoring of the atmosphere) and the EC FP7 NORS (Demonstration Network Of ground-based Remote Sensing Observations in support of the GMES Atmospheric Service, http://nors.aeronomie.be/) projects, a strong focus has been put on tropospheric NO_2 column and profile data product characterization and harmonization, for a limited number of pilot stations. Recent efforts have also been made to intercompare MAXDOAS instruments, in particular during the CINDI campaign (Piters et al., 2012), and to formulate recommendations for SCD retrieval (Roscoe et al., 2010). The inclusion of MAXDOAS instruments in the NDACC network is under progress, following efforts recently done in the NORS project to harmonize and automatize data processing.
The accuracy of the MAXDOAS technique depends on the SCD retrieval noise, the uncertainty on the NO_2 absorption cross-sections and most importantly on the uncertainty of the tropospheric AMF calculation. A summary of all the contributing error sources can be found in Haze et al. (2013). The estimated total error on NO_2 VCD is of the order of 7-17% in polluted conditions (e.g. Irie et al., 2008; Wagner et al., 2011; Hendrick et al., 2014; Kanaya et al., 2014), including both random (around 3 to 10% depending on the instruments) and systematic (11 to 14%) contributions.

2.3 Direct-sun geometry

Direct-sun instruments measure direct sun (ir)radiance during daytime (Figure 1c). The light travels through the whole atmosphere and the measurement is equally sensitive to both troposphere and stratosphere. These instruments therefore provide accurate total column measurements with a minimum of a-priori assumptions.
Although direct-sun measurements have occasionally been performed by MAXDOAS instruments (e.g., BIRA-IASB (Clémer et al., 2008) or AUTH (Kouremeti et al., 2013)), systematic large scale direct-sun observations are currently mostly available from the network of standardized Pandora sun-photometers recently set-up by NASA (Herman et al., 2009, Tzortziou et al., 2013). These instruments have been deployed in about 60 different locations and the network continues to grow. The Pandora spectrometer provides NO_2 vertical column observations with a random uncertainty of about 2.7×10^{14}molec/cm^2 and a systematic uncertainty of 2.7×10^{15} molec/cm^2 (Herman et al., 2009). NO_2 column retrievals from Pandora have been compared to direct-sun multifunction DOAS (MF-DOAS)

and Fourier transform ultraviolet spectrometer (UVFTS) data and have been found to agree to within 12 % (Piters et al., 2012; Wang et al., 2010; Herman et al., 2009).

3. STRATOSPHERIC NO_2 COMPARISONS

The different Zenith-sky instruments used in this study are presented in Figure 2. Data from 15 instruments, mainly located in remote areas, from BIRA-IASB, LATMOS, IUP-Heidelberg and Mainz teams have been collected.

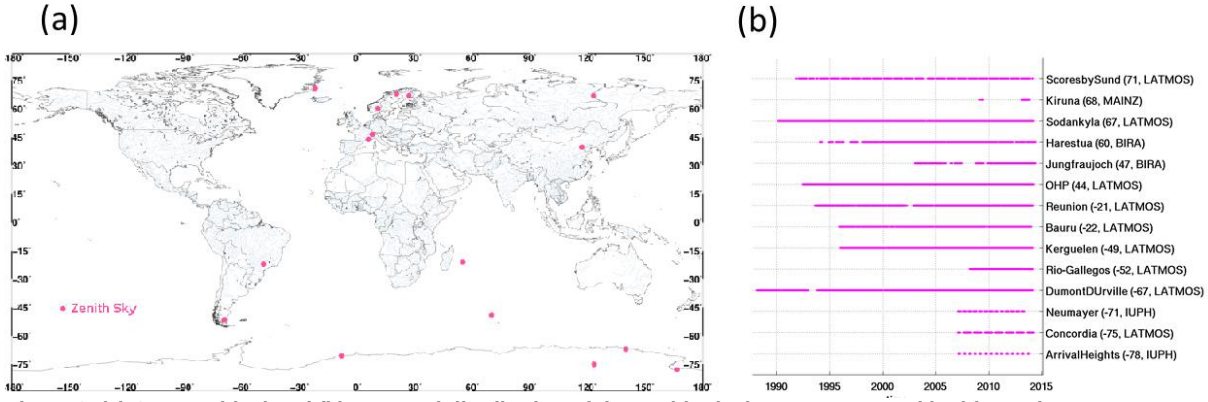

Figure 2: **(a) Geographical and (b) temporal distribution of the zenith-sky instruments used in this study.**

As discussed in Section 2.1, these instruments are part of the NDACC network. Stratospheric NO_2 VCDs are retrieved at twilight using harmonized settings (Van Roozendael and Hendrick, 2012). With a total uncertainty of ≤20%, zenith-sky observations are well suited to validate stratospheric NO_2 columns from nadir UV-vis satellites (see e.g., Ionov et al., 2008; Celarier et al. 2008).

Ground-based validation of stratospheric NO_2 column data requires a dedicated methodology (Lambert et al., 2007). As a prerequisite to accurate comparisons of stratospheric column data, the absence of tropospheric pollution must be ensured through appropriate identification of pollution events and subsequent data filtering. Then, two critical effects leading to temporal and spatial mismatch of the data must be taken into account: the photochemical reactions modifying the partitioning of the nitrogen oxide family slowly during the day and rapidly during twilight, and the progressive geographical displacement and smoothing of the air-mass from which the stratospheric NO_2 information is retrieved, moving and smearing in the direction of the Sun as solar elevation decreases. These effects are presented in Figure 3. Figure 3a shows an example of the diurnal cycle of the stratospheric NO_2 column for a day in April, at 60°N (representative of the Harestua station in Southern Norway) with its rapid decrease and increase of NO_2 at sunrise and sunset and its almost linear increase during the day. Note that this shape of diurnal cycle with full day-night alternance is valid at all low and middle latitudes. At high latitudes, the special photochemistry regimes of polar day and polar night alter significantly the shape of the diurnal cycle. Figure 3b presents an example of the effective stratospheric air-masses measured by the zenith-sky instrument in Izaña, with shifts of the order of a few hundred km towards the direction of the Sun during twilights. Figure 3c presents the relation between the solar zenith angle (SZA) at the station and the effective SZA of the sampled air-mass, that is used to represent the real “photochemical time” of the measurement. For appropriate comparison with satellite data, a correction must be applied to match the two measurement local times. This is done using a NO_2 photochemical correction tool based on look-up tables of the vertically-resolved NO_2 diurnal variation calculated using the photochemical box model PSCBOX (Errera and Fonteyn, 2001). For these calculations, PSCBOX is initialized using SLIMCAT (Chipperfield et al., 1999) chemical fields corresponding to the 2000-2009 period. This covers 18 scenarios of latitude (from 85°N to 85°S by 10° step), 12 months and 24 levels of altitude.

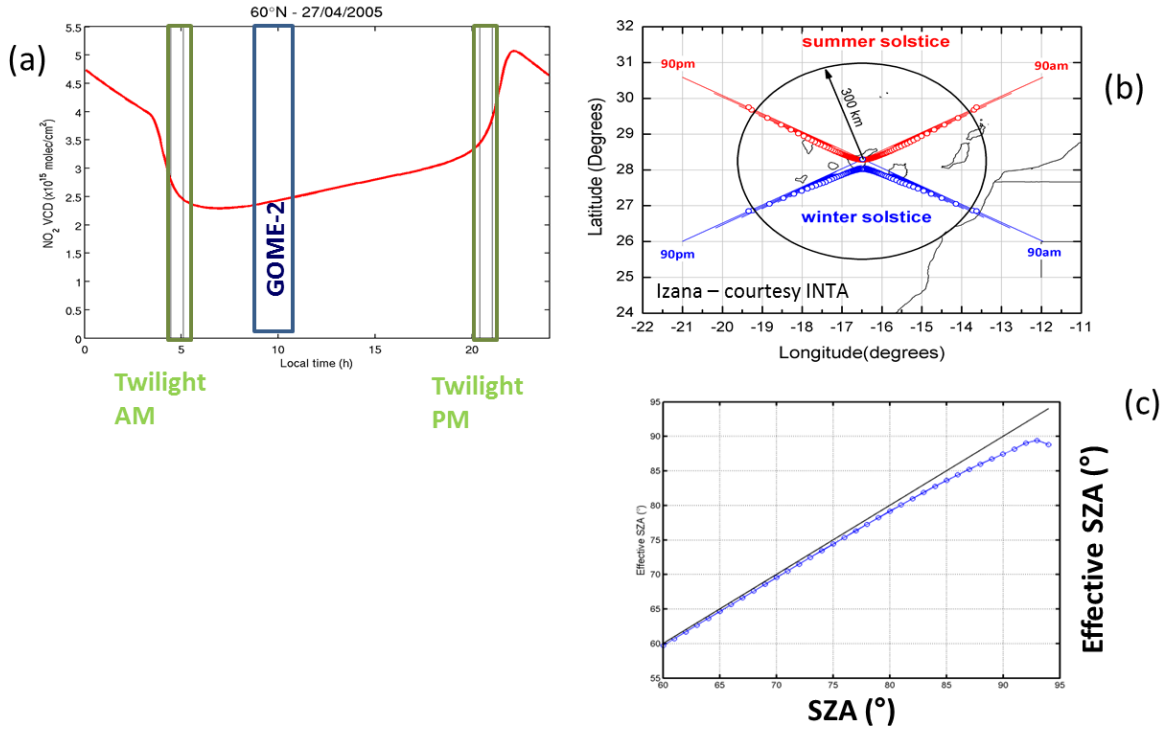

Figure 3: **Different effects to be taken into account for the comparisons of ground-based zenith-sky and satellite nadir NO_2 columns: (a) rapid photochemical variation of stratospheric NO_2, especially at twilight; (b) displacement of the effective air-masses from above the station toward the setting (or rising) sun; (c) relation between the local SZA and the effective SZA at the effective measurement location.**

For the comparison, the GOME-2 GDP data are extracted within 150 km of the different stations listed in Figure 2, and the mean value is calculated for each day. For the ground-based zenith-sky data, the sunrise VCD (considering the effective SZA of the air-masses) are photochemically converted to the satellite overpass SZA of the day. These corrected ground-based NO_2 stratospheric VCD are compared to the satellite column for all common days and monthly means of the daily comparisons are calculated.

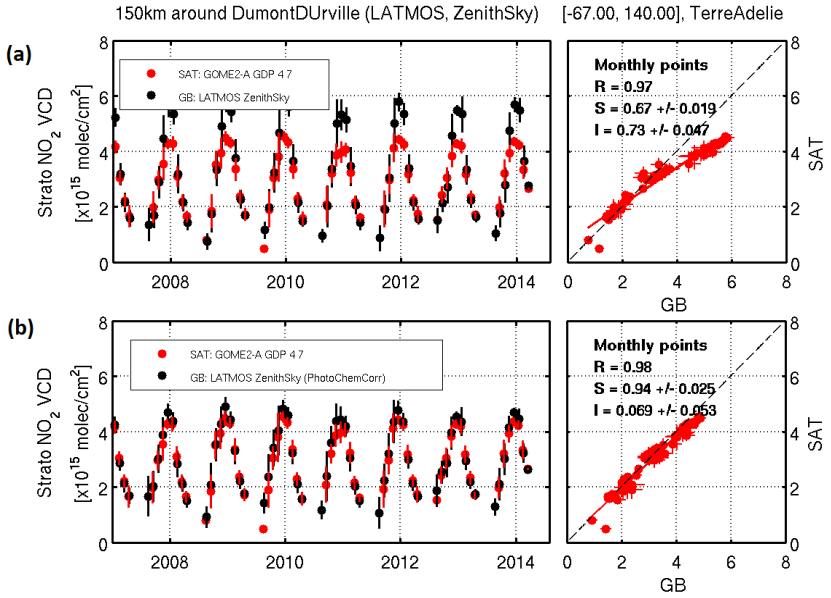

Figure 4: **Stratospheric NO_2 VCD time-series and scatter plot between GOME-2 GDP 4.7 satellite data and LATMOS zenith-sky ground-based data at Dumont d' Urville (-67° latitude, 140° longitude). (a) non corrected and (b) photochemically corrected GB data (see text).**

An example of the monthly mean comparisons is shown in Figure 4 for the Dumont d' Urville SAOZ station (67°S, 140°E). Both (a) un-corrected and (b) photochemically corrected time-series and

correlation plots are shown. The impact of the spatial-temporal mismatch between both measurements appears clearly in panel (a) while the impact of correcting the ground-based data for photochemical effects is well demonstrated in panel (b). The overall impact of the photochemical correction is presented in Figure 5 for all the stations included in the study. One can see that the slope of the orthogonal regression changes from 0.79 to 0.97 when using the photochemical correction, and the intercept is significantly reduced (see values on Figure 5).

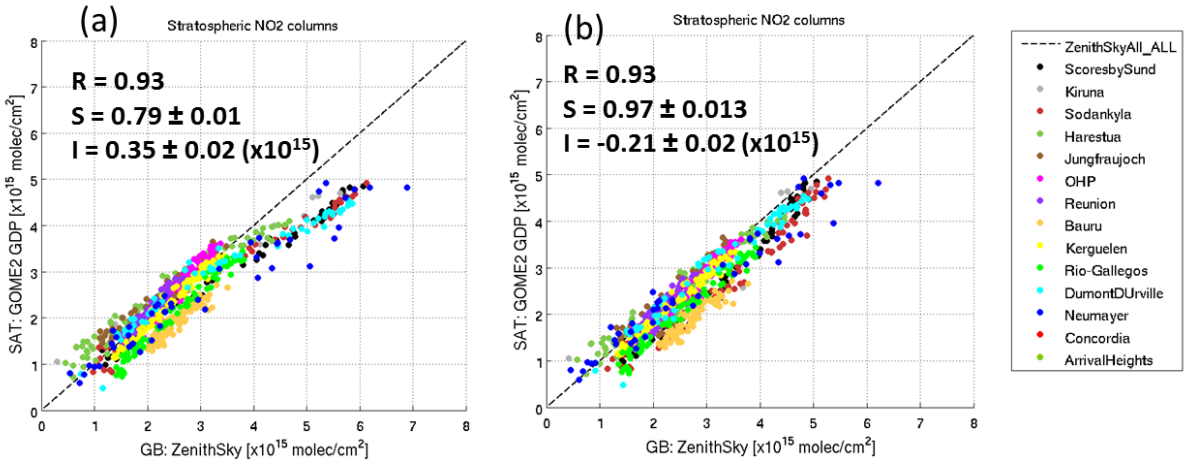

Figure 5: **Stratospheric NO_2 VCD scatter plot between GOME-2 GDP 4.7 satellite data and ZenithSky ground-based data at the 15 stations included in the study. (a) Non corrected and (b) photochemically corrected GB data (see text).**

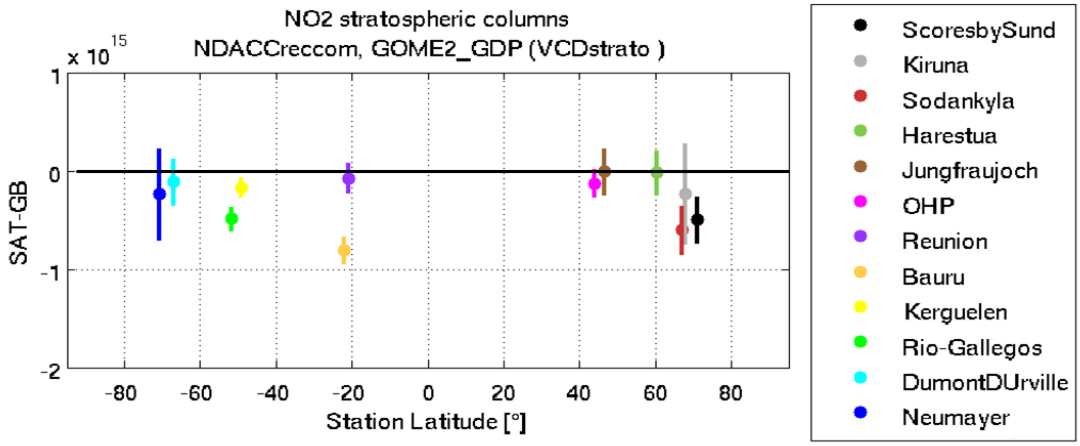

Figure 6: **Stratospheric NO_2 VCD bias (GOME-2 minus GB zenith-sky) at every station over the period 2007-2014, as a function of the station latitudes. The error bars present the temporal variability (the standard deviations over the 01/2007-08/2014 time period).**

Figure 6 presents the latitudinal distribution of the mean bias between GOME-2 and zenith-sky stratospheric NO_2 columns at each station, over the period from January 2007 to August 2014. A good overall agreement is found, with differences of less than $0.5x10^{15}$ molec/cm² for most of the stations. Note that such an agreement is compliant with the requirements on the GOME-2 O3M SAF products (Hovila et al., 2013) which state a target bias of $3\text{-}5x10^{14}$ molec/cm^2 (unpolluted conditions) and a threshold bias of $1x10^{15}$ molec/cm^2. Moreover, these differences are in line with GOME-2 GDP stratospheric column error estimation of 0.15 to $0.3x10^{15}$ molec/cm² as reported by Valks et al. (2011). At a few stations (Rio Gallegos, Bauru, Scoresbysund and Sodankylä) larger differences are observed which might be related to local systematic uncertainties on the spatial filtering approach used in GDP to infer the stratospheric correction. More work is ongoing to better understand the origin of these remaining biases.

4. TROPOSPHERIC NO_2 COMPARISONS

Comparisons of the GOME-2 tropospheric NO_2 columns with MAXDOAS data from OHP, Uccle, Beijing and Xianghe stations have been started as part of the activities of the O3M SAF on the validation of GOME-2 GDP products for both MetOp-A and MetOp-B (Valks et al., 2011; Pinardi et al.,

2011 and Pinardi et al., 2013). For this study, the number of stations has been largely increased by including data from 20 instruments operated by AUTH, BIRA-IASB, Chiba University, IUP-Bremen, IUP-Heidelberg, JAMSTEC, KNMI and Mainz teams. Some of these stations have already been used for satellite validation (Celarier et al., 2008; Brinksma et al., 2008; Vlemmix et al., 2010; Irie et al., 2008, 2012; Lin et al., 2014; Kanaya et al., 2014; Lamsal et al. 2014) but not for the GOME-2 GDP product, and never on a "global scale" like presented here.

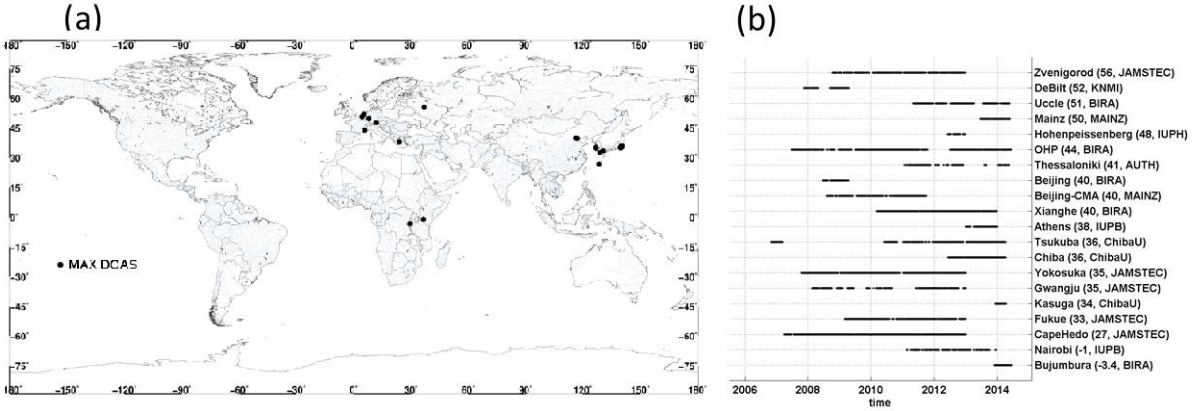

Figure 7: **(a) Geographical and (b) temporal distribution of the MAXDOAS instruments used in this study.**

As briefly discussed in Section 2.2, MAXDOAS instruments used in this study have not been harmonized yet. While recommendations defined during the CINDI campaign for the SCD retrieval (Roscoe et al., 2010) have generally been followed by participants, vertical columns and/or profiles have been obtained using a combination of different approaches. These range from the simple geometrical approximation used to determine vertical columns (Honninger et al., 2004, Brinksma et al., 2008, Ma et al., 2013) to more elaborated profiling algorithms exploiting the full information content of the MAXDOAS technique. Generally speaking, two families of MAXDOAS algorithms coexist currently: (1) vertical profile inversion algorithms using optimal estimation methods (Friess et al., 2006, Clémer et al 2010, Hendrick et al., 2014), and (2) algorithms based on a parameterization of the vertical profile using analytical functions constrained by a few parameters (Irie et al., 2008, Vlemmix et al., 2010, Wagner et al., 2011). Both approaches provide vertical profiles in the 0-4 km altitude range with a DOF between 1.5 and 3. Intercomparison studies are currently ongoing (e.g. Friess et al. 2014, Wittrock et al. 2014, Vlemmix et al., 2014) showing that both approaches lead to consistent results but also to differences in terms of stability and information content extraction (Vlemmix et al., 2014). Details about the retrieval strategy adopted by each partner can be found in Table 1.

Table 1: **Description of the different ground-based NO_2 datasets used in this study and adopted retrieval strategies.**

Group and stations	Retrieval type	Reference
Zenith-sky		
LATMOS: Bauru, Dumont d'Urville, Kerguelen, OHP, Reunion, Rio Gallegos, ScorsbySund, Sodankyla	Stratospheric NO_2 VCD following NDACC recommendations (LATMOS v3)	Pommereau and Goutail, 1988 http://saoz.obs.uvsq.fr/SAOZ_consol_v3.html
IUPH: Arrival Heights, Neumayer	Stratospheric NO_2 VCD following NDACC recommendations	Frieß et al., 2005
MAINZ: Kiruna	Stratospheric NO_2 VCD following NDACC recommendations	Otten et al., 1998; Alliwell et al., 2002
MAXDOAS		
AUTH: Thessaloniki	Tropospheric NO_2 VCD with geom. approx.	Kouremeti et al., 2013
BIRA-IASB: Beijing, Bujumbura, Xianghe, Uccle OHP	Tropospheric NO_2 VCD and profiles with optimal estimation profiling Tropospheric NO_2 VCD with geom. approx.	Clémer et al., 2010; Hendrick et al., 2014
ChibaU: Chiba, Kasuga, Tsukuba	Tropospheric NO_2 VCD and profiles with parameterized profiles	Irie et al., 2011; Irie et al., 2012

IUPB: Athens, Nairobi	Tropospheric NO_2 VCD with geom. approx.	Wittrock et al. 2004
IUPH: Hohenpeissenberg	Tropospheric NO_2 VCD and profiles with optimal estimation profiling	Yilmaz 2012
JAMSTEC: Cape Hedo, Fukue, Gwangju, Yokosuka, Zvernigorod	Tropospheric NO_2 VCD and profiles with parameterized profiles	Kanaya et al., 2014 http://ebcrpa.jamstec.go.jp/maxdoashp/
KNMI: De Bilt	Tropospheric NO_2 VCD with fixed profile shape	Vlemmix et al., 2010
MAINZ: Beijing-CMA, Mainz	Tropospheric NO_2 VCD with geom. approx.	Ma et al., 2013
Direct-sun		
AUTH: Thessaloniki	Total NO_2 VCD	Kouremeti et al., 2013
BIRA-IASB: Beijing, Xianghe	Total NO_2 VCD	Clémer et al., 2010
NASA: Boulder, Busan, Durham, FMI, FourCornersNM, GSFC, Langley, NASA HQ, Oldtown, SERC, Seoul, UHMT	Total NO_2 VCD	Herman et al., 2009, Tzortziou et al., 2013

For the comparison, the GOME-2 GDP data are extracted within 50 km of the different stations listed in Figure 7 and only cloud free pixels (cloud fraction <20%) are selected. The mean value is then calculated for each day. For the ground-based MAXDOAS data, an optional filtering is performed following partners recommendations (on error, cloud flags, color index, etc.) before interpolation at the satellite overpass time. Daily and monthly comparisons are performed.

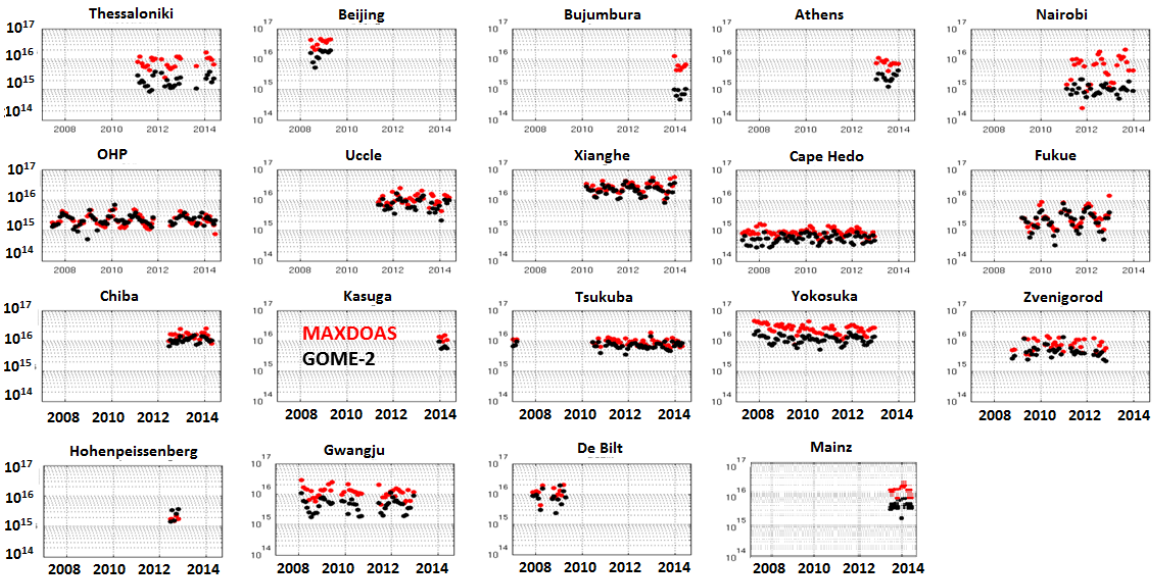

Figure 8: **Tropospheric NO_2 column time series comparison GOME-2 GDP (black) and the ground-based MAXDOAS data (red), between January 2007 and August 2014. The y-axis (the same for every subplot) is a logarithmic scale from $1x10^{14}$ to $1x10^{17}$ molec/cm².**

An example of the time-series of tropospheric NO_2 columns from GOME-2 and MAXDOAS for most of the stations is presented in Figure 8. Pollution episodes are generally well captured by GOME-2 and the monthly averaged comparisons show consistent seasonal variations, with high NO_2 in winter and low NO_2 in summer. Results depend however strongly on the location. While an excellent agreement is obtained for some stations (e.g., Xianghe, OHP, Uccle, Kasuga, De Bilt) larger differences show up at other stations (e.g., Beijing, Yokosuka, Gwangju, Thessaloniki). In such cases, GOME-2 tend to systematically display smaller columns than ground-based MAXDOAS measurements. A closer examination indicates that largest differences are obtained at highly populated urban sites, likely due to the effect of strong local NO_2 emissions seen by ground-based instruments but smeared out at the coarse resolution of the GOME-2 observations (40x80 km^2). One comes to the same conclusion

when inspecting correlation plots representing GOME-2 data against MAXDOAS values for all twenty stations (see Figure 9). As can be seen, results appear to be distributed in groups showing similar behaviors.

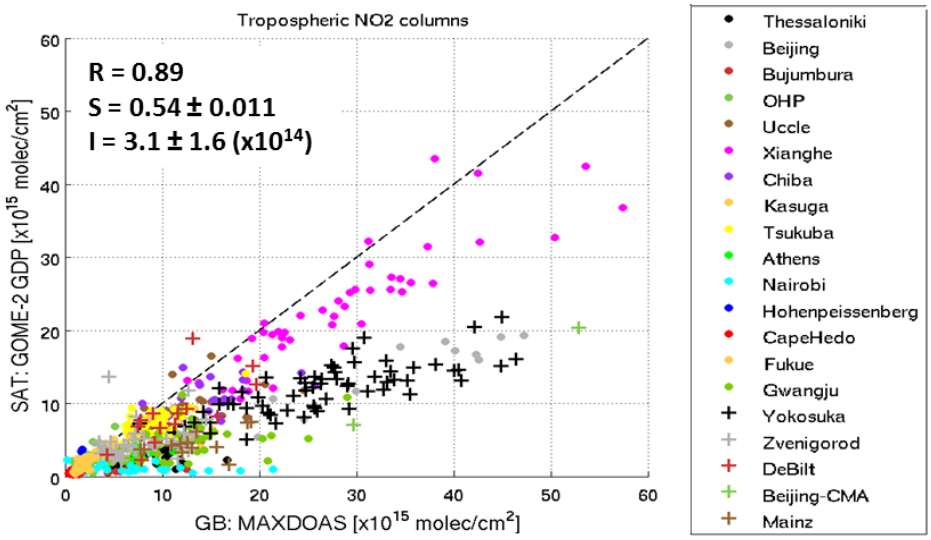

Figure 9: **Tropospheric NO_2 VCD scatter plot between GOME-2 GDP 4.7 satellite data and MAXDOAS ground-based data at the 20 stations included in the study.**

This is better seen in Figure 10 where the stations have been categorized in rural/background, suburban and urban sites. Good agreement is found in suburban and background stations, with slopes around ~0.8 (e.g., Xianghe, Chiba, Tsukuba, Kasuga, Uccle, De Bilt, Hohenpeissenberg, OHP and Cape Hedo) while in urban conditions (Beijing, Yokosuka, Gwangju, Mainz) the MAXDOAS columns are generally much higher than GOME-2 ones. In such cases, the slope of the regression is close to 0.5 in average.

Moreover, some extreme cases are highlighted in Figure 10c (Nairobi, Bujumbura, Thessaloniki and Athens). At these stations, ground-based values are found to be much larger than GOME-2 ones. More work is needed to understand the reasons of such large descrepancies.

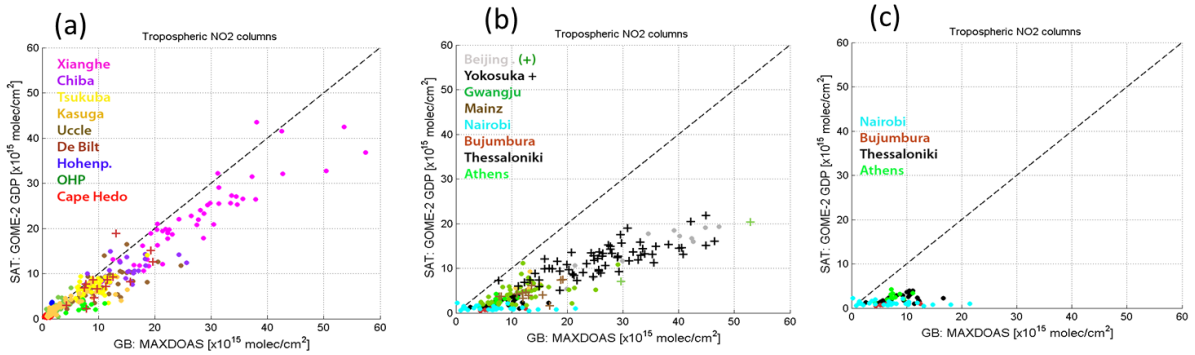

Figure 10: **Same as Figure 9 but dividing into (a) suburban and remote, (b) urban sites and (c) Greece and Africa extreme cases.**

In addition to the expected smearing effect of GOME-2 measurements in urban locations characterized by strong local emissions, one should also consider the possible impact of uncertainties in the applied satellite retrieval assumptions (such as the choices of the a-priori NO_2 profiles, the albedo, the cloud treatment, …). We plan to address this issue by considering the impact of the different vertical sensitivities of the ground-based and satellite measurements, through application of the averaging kernels available from both systems at those stations where NO_2 vertical profiles are retrieved (see Table 1 for details). Another source of discrepancy between ground-based and satellite data sets could be related to the impact of aerosols which can mask or enhance part of the NO_2 detected by the satellite (depending on their altitude relative to the NO_2 layer, see e.g. Kanaya et al. 2014, Lin et al., 2014, Ma et al. 2013). The aerosol information retrieved from the MAXDOAS instruments themselves, or by collocated sunphotometers (e.g. from the AERONET network), will be

exploited in a subsequent phase of the study to investigate the possible impact of such effects on validation results.

5. TOTAL NO_2 COMPARISONS

The different direct-sun instruments used in this study are represented in Figure 11. These include 15 systems mainly located in polluted areas, most of them being Pandora systems operated by NASA. Only Pandora stations having at least 3 months of data have been considered in Figure 11b and in the comparisons presented below.

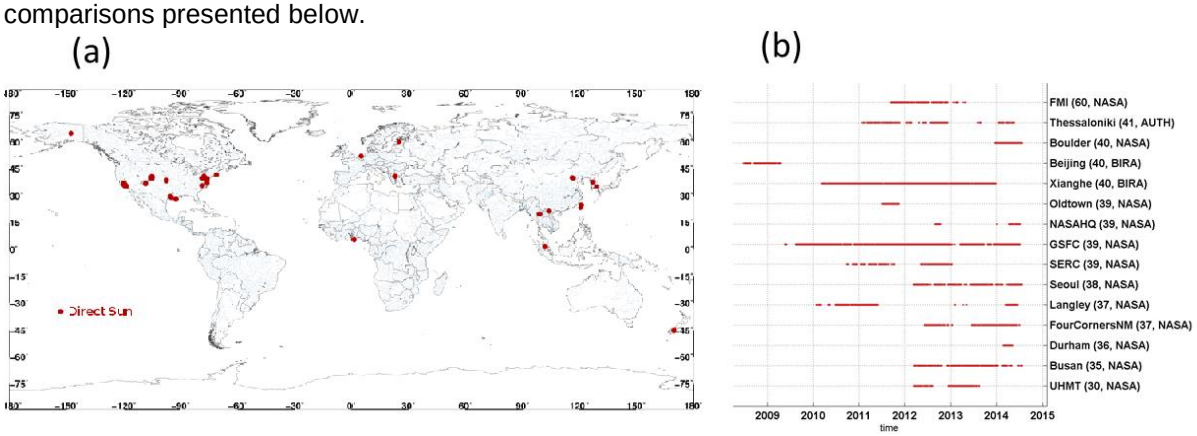

Figure 11: **(a) Geographical and (b) temporal distribution of the direct-sun instruments used in this study. Note that only stations with at least 3 months of data are shown in the time-lines (b).**

As described in Section 2.3, the direct-sun systems allow for accurate total NO_2 column measurements. In this geometry, the main sources of uncertainty are DOAS fit systematic errors, random noise and the estimation of the residual gas amount in the reference spectra. The Pandora systems have nominal accuracy of 2.7×10^{15} molec/cm^2 (Herman et al., 2009) and are thus well-suited to validate total NO_2 columns from nadir UV-vis satellite instruments. Recent validation studies (Tzortziou et al., 2013; Lamsal et al., 2014) compared Pandora data to OMI NO_2 NASA standard product showing the importance of the nature of the Pandora site location for the comparison results.

For the comparison, the GOME-2 GDP data are extracted within 50 km of the different stations and only cloud free pixels (satellite cloud fraction <20%) are selected. For the ground-based direct-sun data, a filtering on error, cloud flags, color index, etc. is performed following recommendations formulated by the Pandora team. The resulting data are interpolated at the satellite overpass time for further comparison.

As for MAXDOAS instruments, the agreement between GOME-2 and ground-based direct-sun measurements is found to be excellent at the suburban site of Xianghe while larger differences are obtained at the urban sites of Beijing, Seoul, Thessaloniki and OldTown. This can be seen in the time-series of Figure 12 and in the scatter plot of Figure 13.

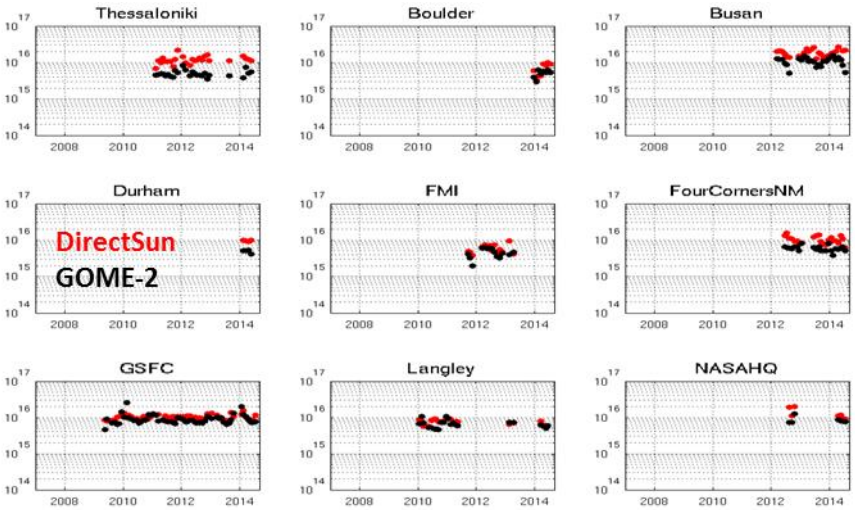

Figure 12: **NO_2 total column time series of GOME-2 GDP (black) and the ground-based direct-sun data (red), between January 2007 and August 2014. The y-axis (the same for every subplot) is a logarithmic scale from $1x10^{14}$ to $1x10^{17}$ molec/cm².**

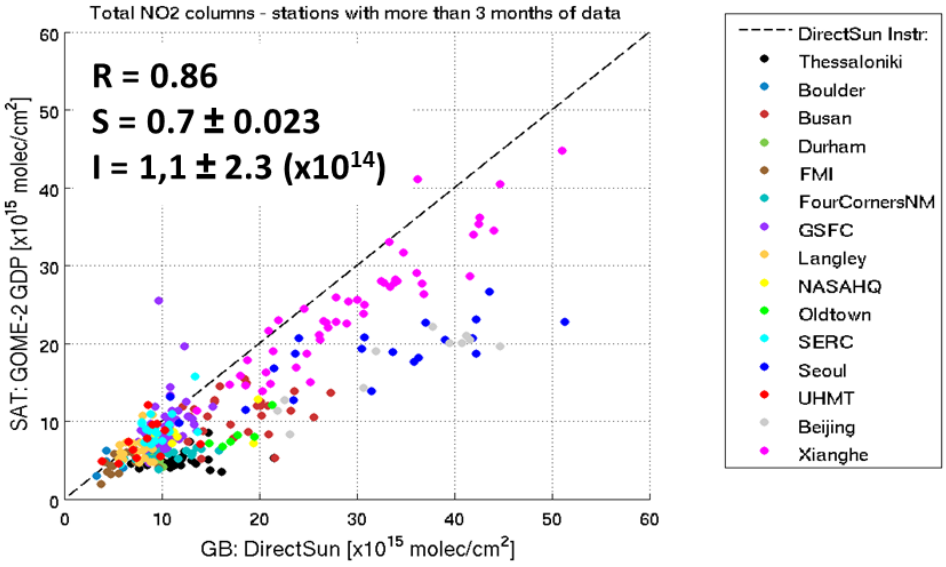

Figure 13: **Total NO_2 VCD scatter plot between GOME-2 GDP 4.7 satellite data and direct-sun ground-based data at the 15 stations (having at least 3 months of data) included in the study.**

A similar impact of the site location was reported in Tzortziou et al. (2013). Likewise, Lamsal et al. (2014) compared OMI and Pandora data from six DISCOVER-AQ campaign basis sites in July 2011 in Maryland and from a long-term site in Langley over the 2010-2012 period. Moderate correlation is found on a daily basis comparison, while when averaging over the whole campaign period, the comparisons improve. The long-term comparison in Langley also shows moderate correlation with different magnitude of the seasonal cycle and some phase differences tentatively explained by the authors as due to the local pollution from traffic and a power plant seen in the Pandora ground-based data.

It is interesting to note the good coherence between the tropospheric and total NO_2 results found for the stations where both MAXDOAS and direct-sun data were operated (Beijing, Xianghe, Thessaloniki). Furthermore, the coherence of the results for megacities is impressive. Very similar results are indeed obtained e.g. for Beijing and Seoul data (see Figure 13).

4. CONCLUSIONS AND FUTURE WORK

In this study data from more than 40 ground-based stations operating DOAS instruments have been used in support of the validation of the GOME-2A GDP NO_2 products over the full MetOp-A mission

(2007 to August 2014). Three major outputs of the GOME-2 NO_2 column processing chain have been studied using a combination of zenith-sky data to validate stratospheric NO_2 content, MAXDOAS data for the tropospheric column and direct-sun data for the total NO_2 column. An advanced tool for the correction of the rapid diurnal variation of stratospheric NO_2 has been used at 15 zenith-sky stations distributed over the globe to remove photochemical time mismatches of the satellite nadir and ground-based zenith-sky measurements.

This study confirms previous results obtained at a limited number of stations before the release of the GOME-2 operational products (Pinardi et al., 2011 and 2013 validation reports). It shows that: (1) stratospheric NO_2 columns are in good agreement with ground-based datasets when photochemical effects are properly taken into account, (2) tropospheric and total NO_2 columns are in good agreement with ground-based data at remote and suburban locations while, for the case of urban sites, GOME-2 NO_2 columns are generally significantly underestimated. No time-dependent degradation of the product is observed in the comparisons.

In the future, we plan to refine the study by using MAXDOAS profile measurements for comparison to GOME-2 data using Averaging Kernels. This will allow to remove the sensitivity of the comparison to the *a-priori* profile used in the satellite retrieval. The extension of the study to MetOp-B data (since July 2013) is also planned. In addition, validation results will be studied as a function of aerosols and meteorological parameters when available, and an improved classification of urban/suburban/remote type of sites will be worked on.

Improved network homogenization and correlative data harmonization are essential requirements for future satellite validation, e.g. in the context of the developing Copernicus Sentinel program. Our study has allowed for a first assessment of the current situation. It is anticipated that progress will be achieved in the near future towards the creation of a global harmonized and quality-controlled network of UV-Vis MAXDOAS and/or direct-sun instruments. This will require continued support to and improved coordination between the relevant developing networks such as NDACC, SAOZ, Pandora, BREDOM, MADRAS etc.

REFERENCES

Aliwell, S.R., P.V. Johnston, A. Richter, M. Van Roozendael, T. Wagner, D.W. Arlander, J.P. Burrows, D.J. Fish, R.L. Jones, K. Karlsen Tornkvist, J.-C. Lambert, K. Pfeilsticker and I. Pundt (2002), Analysis for BrO in zenith-sky spectra - an intercomparison exercise for analysis improvement, J. Geophys. Res., 107, 10.1029/2001JD000329.

Brinksma, E. J., et al. (2008), The 2005 and 2006 DANDELIONS NO2 and aerosol intercomparison campaigns, J. Geophys. Res., 113, D16S46, doi:10.1029/2007JD008808.

Celarier, E. A., E. J. Brinksma, J. F. Gleason, J. P. Veefkind, A. Cede, J. R. Herman, D. Ionov, F. Goutail, J-P. Pommereau, J.-C. Lambert, M. van Roozendael, G. Pinardi, F. Wittrock, A. Schönhardt, A. Richter, O. W. Ibrahim, T. Wagner, B. Bojkov, G. Mount, E. Spinei, C. M. Chen, T. J. Pongetti, S. P. Sander, E. J. Bucsela, M. O. Wenig, D. P. J. Swart, H. Volten, M. Kroon, and P. F. Levelt (2008), Validation of Ozone Monitoring Instrument Nitrogen Dioxide Columns, Journal of Geophysical Research – Atmosphere, Vol. 113, doi:10.1029/2007JD008908.

Chipperfield, M. P. (1999), Multiannual simulations with a threedimensional chemical transport model, J. Geophys. Res., 104 (D1), 1781–1805.

Clémer K., Van Roozendael, M., Fayt, C., Hendrick, F., Hermans, C., Pinardi, G., Spurr, R., Wang, P., and De Mazière, M. (2010), Multiple wavelength retrieval of tropospheric aerosol optical properties from MAXDOAS measurements in Beijing. Atmos. Meas. Tech., **3**, pp 863–878, doi:10.5194/amt-3-863-2010.

Errera, Q. and Fonteyn, D. (2001), Four-dimensional variational chemical assimilation of CRISTA stratospheric measurements, J. Geophys. Res., 106 (D11), 12 253–12 265.

Frieß, U.; Kreher, K.; Johnston, P.V.; Platt, U. (2005), Ground-based DOAS measurements of stratospheric trace gases at two Antarctic stations during the 2002 ozone hole period, Journal of Atmospheric Science, 62, 765–777

Frieß, U., P. S. Monks, J. J. Remedios, A. Rozanov, R. Sinreich, T. Wagner, and U. Platt (2006), MAX-DOAS O4 measurements: A new technique to derive information on atmospheric aerosols: 2. Modeling studies, J. Geophys. Res., 111, D14203, doi:10.1029/2005JD006618.

Friess et al. (2014), Inter-comparison of aerosol extinction profiles retrieved from MAX-DOAS measurements, in preparation.

Haze, F, S. Godin-Beekmann, F. Hendrick, K. Hocke, M. Palm, M. Pastel, A. Richter (2013), NORS Uncertainty Budgets report,D4.3, rev 00- issue of 28/04/2013, http://nors.aeronomie.be/projectdir/PDF/NORS_D4.3_UB.pdf.

Hendrick, F., Müller, J.-F., Clémer, K., Wang, P., De Mazière, M., Fayt, C., Gielen, C., Hermans, C., Ma, J. Z., Pinardi, G., Stavrakou, T., Vlemmix, T., and Van Roozendael, M. (2014), Four years of ground-based MAX-DOAS observations of HONO and NO2 in the Beijing area, Atmos. Chem. Phys., 14, 765-781, doi:10.5194/acp-14-765-2014.

Herman, J., A. Cede, E. Spinei, G. Mount, M. Tzortziou, and N. Abuhassan (2009), NO_2 column amounts from ground-based Pandora and MFDOAS spectrometers using the direct-sun DOAS technique: Inter-comparisons and application to OMI validation, J. Geophys. Res., 114 (D13307), 10.1029/2009JD011848.

Hönninger, G., von Friedeburg, C., and Platt, U. (2004), Multi axis differential optical absorption spectroscopy (MAX-DOAS), Atmos. Chem. Phys., 4, 231-254, doi:10.5194/acp-4-231-2004.

Hovila et al., (2013): O3M SAF Service Specification Document, reference: SAF/O3M/FMI/RQ/ SESP/001, issue: 1.1, 25/11/2013, http://o3msaf.fmi.fi/docs/O3M_SAF_Service_Specification.pdf

Ionov, D. V., Y. M. Timofeyev, V. P. Sinyakov, V. K. Semenov, F. Goutail, J.-P. Pommereau, E. J. Bucsela, E. A. Celarier, and M. Kroon (2008), Ground-based validation of EOS-Aura OMI NO2 vertical column data in the midlatitude mountain ranges of Tien Shan (Kyrgyzstan) and Alps (France). J. Geophys. Res., 113, D15S08, doi:10.1029/2007JD008659.

Irie, H., Kanaya, Y., Akimoto, H., Tanimoto, H., Wang, Z., Gleason, J. F., and Bucsela, E. J. (2008), Validation of OMI tropospheric NO2 column data using MAX-DOAS measurements deep inside the North China Plain in June 2006:Mount Tai Experiment 2006, Atmos. Chem. Phys., 8, 6577–6586, doi:10.5194/acp-8-6577-2008.

Irie, H., Takashima, H., Kanaya, Y., Boersma, K. F., Gast, L., Wittrock, F., Brunner, D., Zhou, Y., and Van Roozendael, M. (2011), Eight-component retrievals from ground-based MAX-DOAS observations, Atmos. Meas. Tech.., 4, 1027-1044 doi:10.5194/amt-4-1027-2011.

Irie, H., Boersma, K. F., Kanaya, Y., Takashima, H., Pan, X., and Wang, Z. F. (2012), Quantitative bias estimates for tropospheric NO_2 columns retrieved from SCIAMACHY, OMI, and GOME-2 using a common standard for East Asia, Atmos. Meas. Tech., 5, 2403-2411, doi:10.5194/amt-5-2403-2012.

Kanaya, Y., Irie, H., Takashima, H., Iwabuchi, H., Akimoto, H., Sudo, K., Gu, M., Chong, J., Kim, Y. J., Lee, H., Li, A., Si, F., Xu, J., Xie, P.-H., Liu, W.-Q., Dzhola, A., Postylyakov, O., Ivanov, V., Grechko, E., Terpugova, S., and Panchenko, M. (2014), Long-term MAX-DOAS network observations of NO2 in Russia and Asia (MADRAS) during the period 2007–2012: instrumentation, elucidation of climatology, and comparisons with OMI satellite observations and global model simulations, Atmos. Chem. Phys., 14, 7909-7927, doi:10.5194/acp-14-7909-2014.

Kouremeti, N., Bais, A. F., Balis, D., and Zyrichidou, I.: Phaethon (2013), A System for the Validation of Satellite Derived Atmospheric Columns of Trace Gases, in Advances in Meteorology, Climatology and Atmospheric Physics, edited by C. G. Helmis and P. T. Nastos, pp. 1081-1088, Springer Berlin Heidelberg.

Lambert, J.-C., I. De Smedt, J. Granville, and P. Valks (2007), Initial Validation of GOME-2 Nitrogen Dioxide Columns (GDP 4.2 OTO/NO2 and NTO/NO2): March-June 2007, IASB/EUMETSAT Technical Note TN-IASB-GOME2-O3MSAF-NO2-01, Issue 1, Revision B, 40 pp., 22 October 2007.

Lamsal, L. N., Krotkov, N. A., Celarier, E. A., Swartz, W. H., Pickering, K. E., Bucsela, E. J., Gleason, J. F., Martin, R. V., Philip, S., Irie, H., Cede, A., Herman, J., Weinheimer, A., Szykman, J. J., and Knepp, T. N. (2014), Evaluation of OMI operational standard NO_2 column retrievals using in situ and surface-based NO_2 observations, Atmos. Chem. Phys., 14, 11587-11609, doi:10.5194/acp-14-11587-2014.

Lin, J.-T., Martin, R. V., Boersma, K. F., Sneep, M., Stammes, P., Spurr, R., Wang, P., Van Roozendael, M., Clémer, K., and Irie, H. (2014), Retrieving tropospheric nitrogen dioxide from the Ozone Monitoring Instrument: effects of aerosols, surface reflectance anisotropy, and vertical profile of nitrogen dioxide, Atmos. Chem. Phys., 14, 1441-1461, doi:10.5194/acp-14-1441-2014, 2014.

Ma, J. Z., Beirle, S., Jin, J. L., Shaiganfar, R., Yan, P., and Wagner, T. (2013), Tropospheric NO_2 vertical column densities over Beijing: results of the first three years of ground-based MAX-DOAS measurements (2008–2011) and satellite validation, Atmos. Chem. Phys., 13, 5629-5629, doi:10.5194/acp-13-5629-2013.

Otten, C., F. Ferlemann, U. Platt, T. Wagner, and K. Pfeilsticker (1998), Groundbased DOAS UV/visible measurements at Kiruna (Sweden) during the SESAME winters 1993/94 and 1994/95, J. of Atm. Chem., 30, 141-162.

Pinardi, G., Lambert, J.C., Granville, J., Clemer, K., Delcloo, A., Hao, N., and P. Valks (2011), MetOp-A GOME-2 GDP 4.3/4.4 total and tropospheric NO2 validation: 2007 – 2010, Technical Note/Validation Report for the EUMETSAT O3MSAF, http://o3msaf.fmi.fi/docs/vr/Validation_ Report_NTO_OTO_NO2_Feb_2011.pdf

Pinardi, G., Lambert, J.-C., Granville, J., Yu, H., De Smedt, I., van Roozendael, M. and Valks, P. (2013), “Interim verification report of GOME-2 GDP 4.7 NO2 column data for MetOp-B Operational Readiness Review”, Technical Note / Validation Report for the EUMETSAT O3MSAF (SAF/O3M/IASB/VR/NO2/095/TN-IASB-GOME2B-O3MSAF-NO2-2013), http://o3msaf.fmi.fi/docs/vr/Validation_Report_NTO_OTO_NO2_Jun_2013.pdf.

Piters, A. J. M., Boersma, K. F., Kroon, M., Hains, J. C., Van Roozendael, M., Wittrock, F., Abuhassan, N., Adams, C., Akrami, M., Allaart, M. A. F., Apituley, A., Beirle, S., Bergwerff, J. B., Berkhout, A. J. C., Brunner, D., Cede, A., Chong, J., Clémer, K., Fayt, C., Frieß, U., Gast, L. F. L., Gil-Ojeda, M., Goutail, F., Graves, R., Griesfeller, A., Großmann, K., Hemerijckx, G., Hendrick, F., Henzing, B., Herman, J., Hermans, C., Hoexum, M., van der Hoff, G. R., Irie, H., Johnston, P. V., Kanaya, Y., Kim, Y. J., Klein Baltink, H., Kreher, K., de Leeuw, G., Leigh, R., Merlaud, A., Moerman, M. M., Monks, P. S., Mount, G. H., Navarro-Comas, M., Oetjen, H., Pazmino, A., Perez-Camacho, M., Peters, E., du Piesanie, A., Pinardi, G., Puentedura, O., Richter, A., Roscoe, H. K., Schönhardt, A., Schwarzenbach, B., Shaiganfar, R., Sluis, W., Spinei, E., Stolk, A. P., Strong, K., Swart, D. P. J., Takashima, H., Vlemmix, T., Vrekoussis, M., Wagner, T., Whyte, C., Wilson, K. M., Yela, M., Yilmaz, S., Zieger, P., and Zhou, Y. (2012), The Cabauw Intercomparison campaign for Nitrogen Dioxide measuring Instruments (CINDI): design, execution, and early results, Atmos. Meas. Tech., 5, 457-485, doi:10.5194/amt-5-457-2012.

Platt, U. and Stutz, J. (2008), Differential Optical Absorption Spectroscopy: Principles and Applications, Springer-Verlag, Berlin, Germany.

Pommereau, J. P., and F. Goutail (1988), O3 and NO2 ground-based measurements by visible spectrometry during Arctic winter and spring 1988, Geophys. Res. Lett., 15(8), 891–894, doi:10.1029/GL015i008p00891.

Richter, A., M. Weber, J. P. Burrows, J.-C. Lambert, and A. van Gijsel (2013), Validation Strategy for Satellite Observations of Tropospheric Reactive Gases, Annals of Geophysics, Vol. 56, 10.4401/AG-6335.

Roscoe, H. K., et al. (1999), Slant column measurements of O3 and NO2 during the NDSC intercomparison of zenith-sky UV-visible spectro- meters in June 1996, J. Atmos. Chem., 32, 281–314, doi:10.1023/ A:1006111216966.

Roscoe, H. K., Van Roozendael, M., Fayt, C., du Piesanie, A., Abuhassan, N., Adams, C., Akrami, M., Cede, A., Chong, J., Clémer, K., Friess, U., Gil Ojeda, M., Goutail, F., Graves, R., Griesfeller, A., Grossmann, K., Hemerijckx, G., Hendrick, F., Herman, J., Hermans, C., Irie, H., Johnston, P. V., Kanaya, Y., Kreher, K., Leigh, R., Merlaud, A., Mount, G. H., Navarro, M., Oetjen, H., Pazmino, A., Perez-Camacho, M., Peters, E., Pinardi, G., Puentedura, O., Richter, A., Schonhardt, A., Shaiganfar, R., Spinei, E., Strong, K., Takashima, H., Vlemmix, T., Vrekoussis, M., Wagner, T., Wittrock, F., Yela, M., Yilmaz, S., Boersma, F., Hains, J., Kroon, M., Piters, A., and Kim, Y. J. (2010), Intercomparison of slant column measurements of NO_2 and O4 by MAX-DOAS and zenith-sky UV and visible spectrometers, Atmos. Meas. Tech., 3, 1629-1646, doi:10.5194/amt-3-1629-2010.

Solomon, S., Schmeltekopf, A. L., and Sanders, R. W. (1987), On the interpretation of zenith sky measurements, J. Geophys. Res., 92, D7, 8311–8319.

Tzortziou M., Herman, J.R., Cede, A., Loughner, C.P., Abuhassa, N., Naik, S. (2013), Spatial and temporal variability of ozone and nitrogen dioxide over a major urban estuarine ecosystem, J. Atmos. Chem., DOI 10.1007/s10874-013-9255-8.

Valks, P., Pinardi, G., Richter, A., Lambert, J.-C., Hao, N., Loyola, D., Van Roozendael, M., and S. Emmadi (2011), Operational total and tropospheric NO2 column retrieval for GOME-2, Atmos. Meas. Tech., 4, pp 1491-1514.

Van Roozendael, M., De Maziere, M., Simon (1994), Ground-based Visible Measurements At The Jungfraujoch Station Since 1990, P. C, J. Quant. Spectrosc. Radiat. Transfer, 52, 231-240.

Van Roozendael, M. and F. Hendrick (2012), http://ndacc-uvvis-wg.aeronomie.be/tools/ NDACC_UVVIS-WG_NO2settings_v4.pdf.

Vandaele, A. C., Fayt, C., Hendrick, F., Hermans, C., Humbled, F., Van Roozendael, M., Gil, M., Navarro, M., Puentedura, O., Yela, M., Braathen, G., Stebel, K., TÃrnkvist, K., Johnston, P., Kreher, K., Goutail, F., Mieville, A., Pommereau, J.-P., Khaikine, S., Richter, A., Oetjen, H., Wittrock, F., Bugarski, S., Friess, U., Pfeilsticker, K., Sinreich, R., Wagner, T., Corlett, G., and Leigh, R. (2005), An intercomparison campaign of ground-based UV-visible measurements of NO2, BrO, and OClO slant columns: Methods of analysis and results for NO2, J. Geophys. Res., 110, D08305, doi:10.1029/ 2004JD005423.

Vlemmix, T., Piters, A. J. M., Stammes, P., Wang, P., and Levelt, P. F. (2010), Retrieval of tropospheric NO_2 using the MAX-DOAS method combined with relative intensity measurements for aerosol correction, Atmos. Meas. Tech., 3, 1287-1305, doi:10.5194/amt-3-1287-2010.

Vlemmix, T., Piters, A. J. M., Berkhout, A. J. C., Gast, L. F. L., Wang, P., and Levelt, P. F. (2011), Ability of the MAX-DOAS method to derive profile information for NO_2: can the boundary layer and free troposphere be separated?, Atmos. Meas. Tech., 4, 2659-2684, doi:10.5194/amt-4-2659-2011.

Vlemmix, T., Hendrick, F., Pinardi, G., De Smedt, I., Fayt, C., Hermans, C., Piters, A., Levelt, P., and Van Roozendael, M. (2014), MAX-DOAS observations of aerosols, formaldehyde and nitrogen dioxide in the Beijing area: comparison of two profile retrieval approaches, Atmos. Meas. Tech. Discuss., 7, 9673-9731, doi:10.5194/amtd-7-9673-2014.

Wagner, T., Beirle, S., Brauers, T., Deutschmann, T., Frieß, U., Hak, C., Halla, J. D., Heue, K. P., Junkermann, W., Li, X., Platt, U., and Pundt-Gruber, I. (2011), Inversion of tropospheric profiles of aerosol extinction and HCHO and NO2 mixing ratios from MAX-DOAS observations in Milano during the summer of 2003 and comparison with independent data sets, Atmos. Meas. Tech., 4, 2685-2715, doi:10.5194/amt-4-2685-2011.

Wang, S., Pongetti, T. J., Sander, S. P., Spinei, E., Mount, G. H., Cede, A., and Herman, J. (2010), Direct sun measurements of NO2 column abundances from Table Mountain, California:

intercomparison of low- and high-resolution spectrometers, J. Geophys. Res., 115, D13305, doi:10.1029/2009JD013503.

Wittrock, F., Oetjen, H., Richter, A., Fietkau, S., Medeke, T., Rozanov, A., and Burrows, J.P. (2004), MAX-DOAS measurements of atmospheric trace gases in Ny-Alesund – Radiative transfer studies and their application, Atmos. Chem. Phys., 4, 955–966, doi:10.5194/acp-4-955-2004.

Wittrock et al. (2014), Measurements of NO_2 profiles with MAX-DOAS: Theoretical and practical case studies as part of the Cabauw Intercomparison campaign for Nitrogen Dioxide Measuring Instruments (CINDI), in preparation.

Yilmaz, S (2012), Retrieval of Atmospheric Aerosol and Trace Gas Vertical Profiles using Multi-Axis Differential Optical Absorption Spectroscopy, Dissertation, University of Heidelberg.

ACKNOWLEDGEMENT

This work has been funded by EUMETSAT through the first and second phases of the O3M-SAF Continuous Development and Operations Phase (CDOP-1/2), and by the Belgian Federal Science Policy Office (BELSPO) via the ProDEx SECPEA, A3C and ACROSAT projects.